# Passive permanent magnet bearings for rotating shaft : Analytical calculation

Valerie Lemarquand[*]
*LAPLACE. UMR5213. Universite de Toulouse*
*France*

Guy Lemarquand[†]
*LAUM. UMR6613. Universite du Maine*
*France*

## 1. Introduction

Magnetic bearings are contactless suspension devices, which are mainly used for rotating applications but also exist for translational ones. Their major interest lies of course in the fact that there is no contact and therefore no friction at all between the rotating part and its support. As a consequence, these bearings allow very high rotational speeds. Such devices have been investigated for eighty years. Let's remind the works of F. Holmes and J. Beams (Holmes & Beams, 1937) for centrifuges.

The appearing of modern rare earth permanent magnets allowed the developments of passive devices, in which magnets work in repulsion (Meeks, 1974)(Yonnet, 1978).

Furthermore, as passive magnetic bearings don't require any lubricant they can be used in vacuum and in very clean environments.

Their main applications are high speed systems such as turbo-molecular pumps, turbo-compressors, energy storage flywheels, high-speed machine tool spindles, ultra-centrifuges and they are used in watt-hour meters and other systems in which a very low friction is required too (Hussien et al., 2005)(Filatov & Maslen, 2001).

The magnetic levitation of a rotor requires the control of five degrees of freedom. The sixth degree of freedom corresponds to the principal rotation about the motor axis. As a consequence of the Earnshaw's theorem, at least one of the axes has to be controlled actively. For example, in the case of a discoidal wheel, three axes can be controlled by passive bearings and two axes have to be controlled actively (Lemarquand & Yonnet, 1998). Moreover, in some cases the motor itself can be designed to fulfil the function of an active bearing (Barthod & Lemarquand, 1995). Passive magnetic bearings are simple contactless suspension devices but it must be emphazised that one bearing controls a single degree of freedom. Moreover, it exerts only a stiffness on this degree of freedom and no damping.

---

[*]valerie.lemarquand@ieee.org
[†]guy.lemarquand@ieee.org

Permanent magnet bearings for rotating shafts are constituted of ring permanent magnets. The simplest structure consists either of two concentric rings separated by a cylindrical air gap or of two rings of same dimensions separated by a plane air gap. Depending on the magnet magnetization directions, the devices work as axial or radial bearings and thus control the position along an axis or the centering of an axis. The several possible configurations are discussed throughout this chapter. The point is that in each case the basic part is a ring magnet. Therefore, the values of importance are the magnetic field created by such a ring magnet, the force exerted between two ring magnets and the stiffness associated.

The first author who carried out analytical calculations of the magnetic field created by ring permanent magnets is Durand (Durand, 1968). More recently, many authors proposed simplified and robust formulations of the three components of the magnetic field created by ring permanent magnets (Ravaud et al., 2008)(Ravaud, Lemarquand, Lemarquand & Depollier, 2009)(Babic & Akyel, 2008a)(Babic & Akyel, 2008b)(Azzerboni & Cardelli, 1993).
Moreover, the evaluation of the magnetic field created by ring magnets is only a helpful step in the process of the force calculation. Indeed, the force and the stiffness are the values of importance for the design and optimization of a bearing. So, authors have tried to work out analytical expressions of the force exerted between two ring permanent magnets (Kim et al., 1997)(Lang, 2002)(Samanta & Hirani, 2008)(Janssen et al., 2010)(Azukizawa et al., 2008).
This chapter intends to give a detailed description of the modelling and approach used to calculate analytically the force and the stiffness between two ring permanent magnets with axial or radial polarizations (Ravaud, Lemarquand & Lemarquand, 2009a)(Ravaud, Lemarquand & Lemarquand, 2009b). Then, these formulations will be used to study magnetic bearings structures and their properties.

## 2. Analytical determination of the force transmitted between two axially polarized ring permanent magnets.

### 2.1 Preliminary remark

The first structure considered is shown on Fig.1. It is constituted of two concentric axially magnetized ring permanent magnets. When the polarization directions of the rings are antiparallel, as on the figure, the bearing controls the axial position of the rotor and works as a so called axial bearing. When the polarization directions are the same, then the device controls the centering around the axis and works as a so called radial bearing. Only one of the two configurations will be studied thoroughly in this chapter because the results of the second one are easily deducted from the first one. Indeed, the difference between the configurations consists in the change of one of the polarization direction into its opposite. The consequence is a simple change of sign in all the results for the axial force and for the axial stiffness which are the values that will be calculated.

Furthermore, the stiffness in the controlled direction is often considered to be the most interesting value in a bearing. So, for an axial bearing, the axial stiffness is the point. Nevertheless, both stiffnesses are linked. Indeed, when the rings are in their centered position, for symmetry reasons, the axial stiffness, $K_z$, and the radial one, $K_r$, verify:

$$2K_r + K_z = 0 \qquad (1)$$

So, either the axial or the radial force may be calculated and is sufficient to deduct both stiffnesses. Thus, the choice was made for this chapter to present only the axial force and stiffness in the sections dealing with axially polarized magnets.
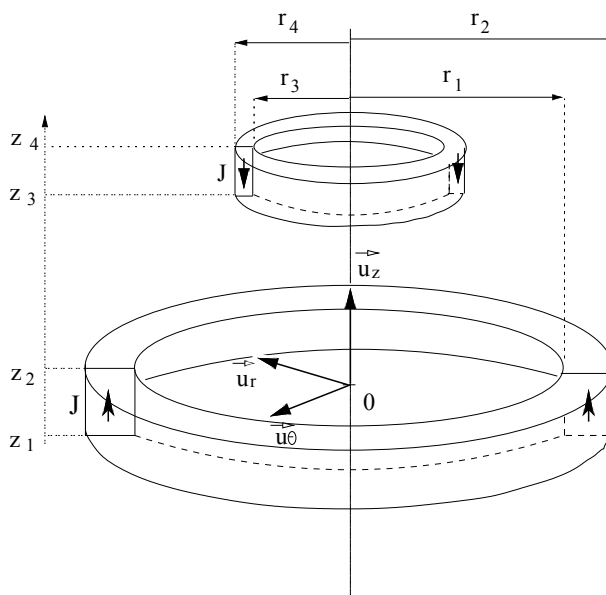
Fig. 1. Axial bearing constituted of two axially magnetized ring permanent magnets. $J_1$ and $J_2$ are the magnet polarizations

### 2.2 Notations

The parameters which describe the geometry of Fig.1 and its properties are listed below:

$J_1$: outer ring polarization [T].

$J_2$: inner ring polarization [T].

$r_1$, $r_2$: radial coordinates of the outer ring [m].

$r_3$, $r_4$: radial coordinates of the inner ring [m].

$z_1$, $z_2$: axial coordinates of the outer ring [m].

$z_3$, $z_4$: axial coordinates of the inner ring [m].

$h_1 = z_2 - z_1$: outer ring height [m].

$h_2 = z_4 - z_3$: inner ring height [m].

The rings are radially centered and their polarizations are supposed to be uniform.

### 2.3 Magnet modelling

The axially polarized ring magnet has to be modelled and two approaches are available to do so. Indeed, the magnet can have a coulombian representation, with fictitious magnetic charges or an amperian one, with current densities. In the latter, the magnet is modelled by two cylindrical surface current densities $k_1$ and $k_2$ located on the inner and outer lateral surfaces of the ring whereas in the former the magnet is modelled by two surface charge densities located on the plane top and bottom faces of the ring.

As a remark, the choice of the model doesn't depend on the nature of the real magnetic source, but is done to obtain an analytical formulation. Indeed, the authors have demontrated
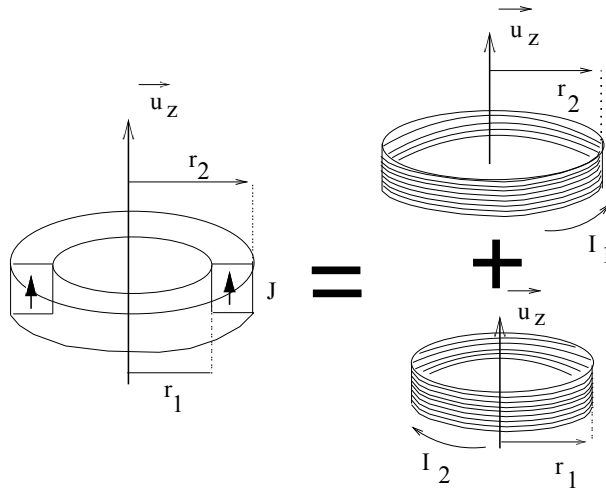
Fig. 2. Model of a ring magnet: amperian equivalence.

that depending on the polarization direction of the source only one of the model generally yields an analytical formulation. So, the choice rather depends on the considered problem.

### 2.4 Force calculation

The force transmitted between two axially polarized ring permanent magnets is determined by using the amperian approach. Thus, each ring is replaced by two coils of $N_1$ and $N_2$ turns in which two currents, $I_1$ and $I_2$, flow. Indeed, a ring magnet whose polarization is axial and points up, with an inner radius $r_1$ and an outer one $r_2$, can be modelled by a coil of radius $r_2$ with a current $I_2$ flowing anticlockwise and a coil of radius $r_1$ with a current $I_1$ flowing clockwise (Fig.2).

The equivalent surface current densities related to the coil heights $h_1$ and $h_2$ are defined as follows for the calculations:

$k_1 = N_1 I_1 / h_1$: equivalent surface current density for the coils of radii $r_1$ and $r_2$.
$k_2 = N_2 I_2 / h_2$: equivalent surface current density for the coils of radii $r_3$ and $r_4$.

The axial force, $F_z$, created between the two ring magnets is given by:

$$F_z = \frac{\mu_0 k_1 k_2}{2} \sum_{i=1}^{2} \sum_{j=3}^{4} (-1)^{1+i+j} \left\{ f_z(r_i, r_j) \right\} \tag{2}$$

with

$$f_z(r_i, r_j) = r_i r_j \int_{z_3}^{z_4} \int_{z_1}^{z_2} \int_{0}^{2\pi} \frac{(\tilde{\tilde{z}} - \tilde{z}) \cos(\tilde{\theta}) d\tilde{z} d\tilde{\tilde{z}} d\tilde{\theta}}{\left( r_i^2 + r_j^2 - 2 r_i r_j \cos(\tilde{\theta}) + (\tilde{\tilde{z}} - \tilde{z})^2 \right)^{\frac{3}{2}}}$$

| Parameter | Definition |
|-----------|------------|
| $\beta$ | $\frac{b+c}{b-c}$ |
| $\mu$ | $\frac{c}{b+c}$ |
| $\epsilon$ | $\frac{c}{c-b}$ |

Table 1. Parameters in the analytical expression of the force exerted between two axially polarized ring magnets.

The current densities are linked to the magnet polarizations by:

$$k_1 = \frac{J_1}{\mu_0} \tag{3}$$

and

$$k_2 = \frac{J_2}{\mu_0} \tag{4}$$

Then the axial force becomes:

$$F_z = \frac{J_1 J_2}{2\mu_0} \sum_{i,k=1}^{2} \sum_{j,l=3}^{4} (-1)^{(1+i+j+k+l)} F_{i,j,k,l} \tag{5}$$

with

$$F_{i,j,k,l} = r_i r_j g \left( z_k - z_l, r_i^2 + r_j^2 + (z_k - z_l)^2, -2r_i r_j \right) \tag{6}$$

$$g(a,b,c) = A + S$$

$$A = \frac{a^2 - b}{c}\pi + \frac{\sqrt{c^2 - (a^2 - b)^2}}{c}\left( \log\left[ \frac{-16c^2}{(c^2 - (a^2 - b)^2)^{(\frac{3}{2})}} \right] + \log\left[ \frac{c^2}{(c^2 - (a^2 - b)^2)^{(\frac{3}{2})}} \right]\right)$$

$$\begin{aligned}
S = \ & \frac{2ia}{c\sqrt{b+c}}\left( (b+c)\mathbf{E}\left[ \arcsin\left[ \sqrt{\beta}, \beta^{-1} \right] \right] - c\mathbf{F}\left[ \arcsin\left[ \sqrt{\beta}, \beta^{-1} \right] \right]\right) \\
& + \frac{2a}{c\sqrt{b} - c\sqrt{\epsilon}}\left( \frac{c}{\sqrt{\mu}}\mathbf{E}\left[ \beta^{-1} \right] - c\sqrt{\mu}\mathbf{K}\left[ \beta^{-1} \right]\right) \\
& + \sqrt{\epsilon\beta^{-1}}\left( (b - a^2)\mathbf{K}\left[ 2\mu \right] + (a^2 - b + c)\mathbf{\Pi}\left[ \frac{2c}{b+c-a^2}, 2\mu \right]\right)
\end{aligned} \tag{7}$$

The special functions used are defined as follows:
$\mathbf{K}[m]$ is the complete elliptic integral of the first kind.

$$\mathbf{K}[m] = \int_0^{\frac{\pi}{2}} \frac{1}{\sqrt{1 - m\sin(\theta)^2}} d\theta \tag{8}$$

$\mathbf{F}[\phi, m]$ is the incomplete elliptic integral of the first kind.

$$\mathbf{F}[\phi, m] = \int_0^\phi \frac{1}{\sqrt{1 - m\sin(\theta)^2}} d\theta \tag{9}$$

$\mathbf{E}[\phi, m]$ is the incomplete elliptic integral of the second kind.

$$\mathbf{E}[\phi, m] = \int_0^\phi \sqrt{1 - m\sin(\theta)^2} d\theta \tag{10}$$

$$\mathbf{E}[m] = \int_0^{\frac{\pi}{2}} \sqrt{1 - m\sin(\theta)^2} d\theta \tag{11}$$

$\mathbf{\Pi}[n, m]$ is the incomplete elliptic integral of the third kind.

$$\mathbf{\Pi}[n, m] = \mathbf{\Pi}\left[n, \frac{\pi}{2}, m\right] \tag{12}$$

with

$$\mathbf{\Pi}[n, \phi, m] = \int_0^\phi \frac{1}{\sqrt{1 - n\sin(\theta)^2}} \frac{1}{\sqrt{1 - m\sin(\theta)^2}} d\theta \tag{13}$$

## 3. Exact analytical formulation of the axial stiffness between two axially polarized ring magnets.

The axial stiffness, $K_z$ existing between two axially polarized ring magnets can be calculated by deriving the axial force transmitted between the two rings, $F_z$, with regard to the axial displacement, $z$:

$$K_z = -\frac{d}{dz} F_z \tag{14}$$

$F_z$ is replaced by the integral formulation of Eq.5 and after some mathematical manipulations the axial stiffness can be written:

$$K_z = \frac{J_1 J_2}{2\mu_0} \sum_{i,k=1}^2 \sum_{j,l=3}^4 (-1)^{(1+i+j+k+l)} C_{i,j,k,l} \tag{15}$$

where

$$
\begin{aligned}
C_{i,j,k,l} &= 2\sqrt{\alpha}\mathbf{E}\left[\frac{-4r_i r_j}{\alpha}\right] - 2\frac{r_i^2 + r_j^2 + (z_k - z_l)^2}{\sqrt{\alpha}} \mathbf{K}\left[\frac{-4r_i r_j}{\alpha}\right] \\
\alpha &= (r_i - r_j)^2 + (z_k - z_l)^2
\end{aligned}
\tag{16}
$$

## 4. Study and characteristics of axial bearings with axially polarized ring magnets and a cylindrical air gap.

### 4.1 Structures with two ring magnets

This section considers devices constituted of two ring magnets with antiparallel polarization directions. So, the devices work as axial bearings. The influence of the different parameters of the geometry on both the axial force and stiffness is studied.

### 4.1.1 Geometry

The device geometry is shown on Fig.1. The radii remain the same as previously defined. Both ring magnets have the same axial dimension, the height $h_1 = h_2 = h$. The axial coordinate, $z$, characterizes the axial displacement of the inner ring with regard to the outer one. The polarization of the magnets is equal to $1T$.

The initial set of dimensions for each study is the following:

$r_1 = 25mm, r_2 = 28mm, r_3 = 21mm, r_4 = 24mm, h = 3mm$

Thus the initial air gap is $1mm$ wide and the ring magnets have an initial square cross section of $3 \times 3mm^2$.

### 4.1.2 Air gap influence

The ring cross section is kept constant and the radial dimension of the air gap, $r_1 - r_3$, is varied by modifying the radii of the inner ring. Fig.3 and 4 show how the axial force and stiffness are modified when the axial inner ring position changes for different values of the air gap.

Naturally, when the air gap decreases, the modulus of the axial force for a given axial position of the inner ring increases (except for large displacements) and so does the modulus of the axial stiffness. Furthermore, it has to be noted that a positive stiffness corresponds to a stable configuration in which the force is a pull-back one, whereas a negative stiffness corresponds to an unstable position: the inner ring gets ejected!
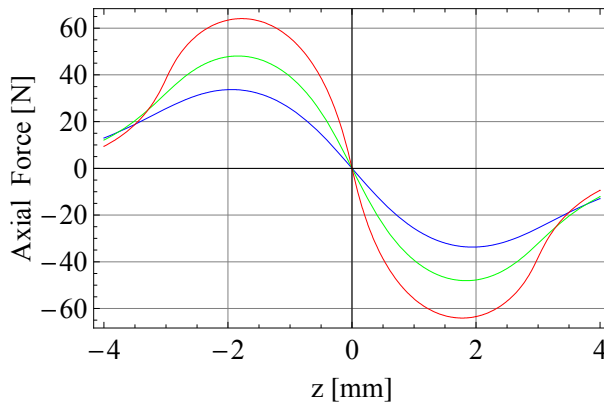


Fig. 3. Axial force for several air gap radial dimensions. Blue: $r_1 = 25mm, r_2 = 28mm, r_3 = 21mm, r_4 = 24mm, h = 3mm$ Air gap $1mm$, Green: Air gap $0.5mm$ , Red: Air gap $0.1mm$

### 4.1.3 Ring height influence

The air gap is kept constant as well as the ring radii and the height of the rings is varied. Fig.5 and 6 show how the axial force and stiffness are modified. When the magnet height decreases, the modulus of the axial force for a given axial position of the inner ring decreases. This is normal, as the magnet volume also decreases.

The study of the stiffness is carried out for decreasing ring heights (Fig.6) but also for increasing ones (Fig.7). As a result, the stiffness doesn't go on increasing in a significant way above a given ring height. This means that increasing the magnet height, and consequently
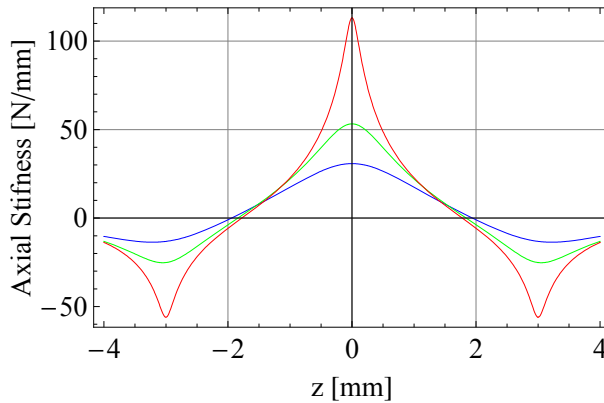
Fig. 4. Axial stiffness for several air gap radial dimensions. Blue: $r_1 = 25mm, r_2 = 28mm, r_3 = 21mm, r_4 = 24mm, h = 3mm$ Air gap $1mm$, Green: Air gap $0.5mm$ , Red: Air gap $0.1mm$

the magnet volume, above a given value isn't interesting to increase the stiffness. Moreover, it has to be noted that when the height is reduced by half, from $3mm$ to $1.5mm$, the stiffness is only reduced by a third. This points out that in this configuration, the loss on the stiffness isn't that bad whereas the gain in volume is really interesting. This result will be useful for other kinds of bearing structures -stacked structures- in a further section. Besides, the magnet height shouln't become smaller than the half of its radial thickness unless the demagnetizing field inside the magnet becomes too strong and demagnetizes it.
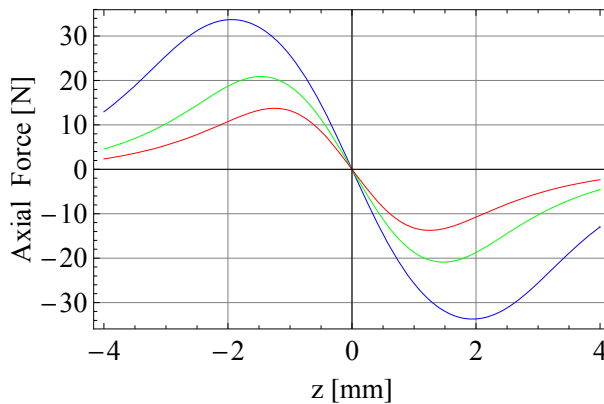

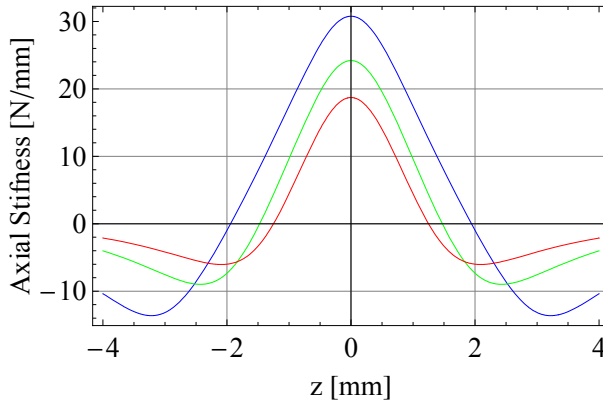
Fig. 5. Axial force for ring small heights. Blue: $r_1 = 25mm, r_2 = 28mm, r_3 = 21mm, r_4 = 24mm$, air gap $1mm$ $h = 3mm$, Green: $h = 2mm$ , Red: $h = 1.5mm$.

### 4.1.4 Ring radial thickness influence
Now, the radial thickness of the ring magnets is varied. The ring height, $h = 3mm$, and the air gap length, $1mm$, are kept constant and the outer radius of the outer ring, $r_2$, is increased of

Fig. 6. Axial stiffness for ring small heights. Blue: $r_1 = 25mm, r_2 = 28mm, r_3 = 21mm, r_4 = 24mm$, air gap $1mm$ $h = 3mm$, Green: $h = 2mm$ , Red: $h = 1.5mm$.
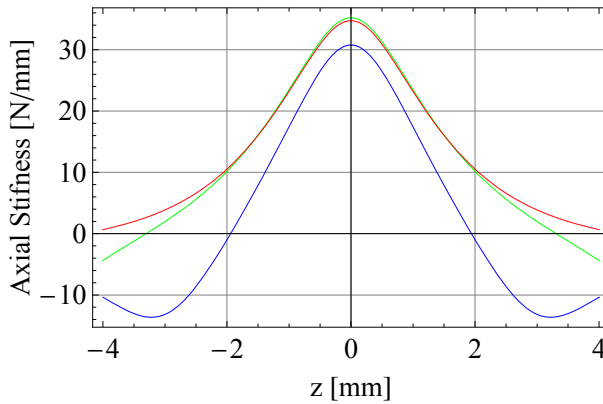


Fig. 7. Axial stiffness for ring large heights. Blue: $r_1 = 25mm, r_2 = 28mm, r_3 = 21mm, r_4 = 24mm$, air gap $1mm$ $h = 3mm$, Green: $h = 6mm$ , Red: $h = 9mm$.

the same quantity as the inner radius of the inner ring, $r_3$, is decreased. So, the inner ring has always the same radial thickness as the outer one.

When the radial thickness increases, the modulus of the axial force for a given axial displacement of the inner ring also increases (Fig.8). This behavior is expected as once again the magnet volume increases. However, the ring thickness doesn't seem a very sensitive parameter. Indeed, the variation isn't as dramatic as with the previous studied parameters.

### 4.1.5 Ring mean perimeter influence

The outer ring perimeter is varied and all the radii are varied to keep the ring cross section and the air gap constant. As a result, when the device perimeter -or the air gap perimeter-increases, the modulus of the axial force for a given axial displacement of the inner ring also
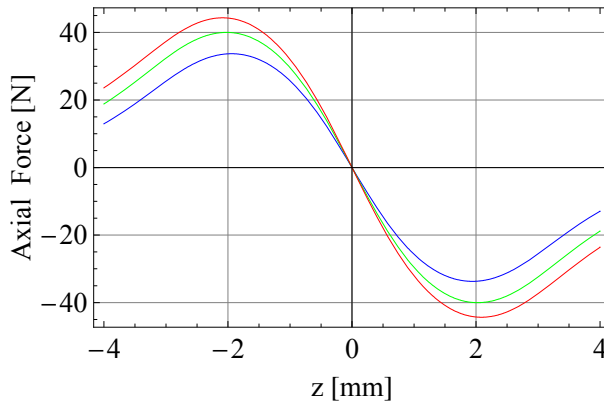
Fig. 8. Axial force for several radial thicknesses. Blue: $r_1 = 25mm, r_2 = 28mm, r_3 = 21mm, r_4 = 24mm$, $h = 3mm$, air gap $1mm$, Radial thickness $r_2 - r_1 = r_4 - r_3 = 3mm$, Green: $4mm$ , Red: $5mm$.

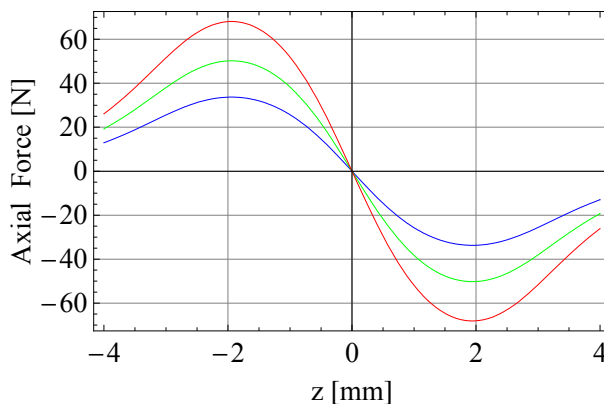increases (Fig.9). This result is expected as the magnet volume also increases.



Fig. 9. Axial force for several air gap perimeters. $h = 3mm$, air gap $1mm$. Blue: $r_1 = 25mm, r_2 = 28mm, r_3 = 21mm, r_4 = 24mm$. Green: $r_1 = 37mm, r_2 = 40mm, r_3 = 33mm, r_4 = 36mm$. Red: $r_1 = 50mm, r_2 = 53mm, r_3 = 46mm, r_4 = 49mm$.

### 4.1.6 Maximum axial force

Previous results are interesting as they show the shape of the axial force and stiffness when different dimensional parameters are varied. Nevertheless, it is necessary to complete these results with additional studies, such as the study of the maximum force for example, in order to compare them. Indeed, a general conclusion is that the axial force increases when the magnet volume increases, but the way it increases depends on the parameter which makes the volume increase.

So, the blue line on Fig.10 shows that the maximum force varies linearly with the air gap diameter. Furthermore, this variation is also linear for radially thicker ring magnets (green and red lines on Fig.10).

As a conclusion, the maximum axial force, and the axial stiffness too, is proportional to the air gap diameter, as long as this diameter isn't too small (which means above 5mm).
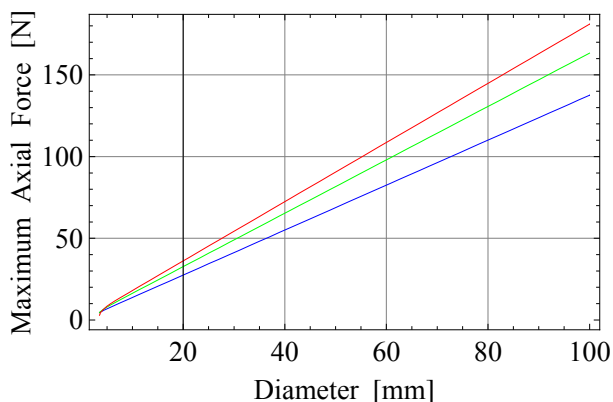


Fig. 10. Maximum axial force versus the air gap perimeter for several ring radial thicknesses. Air gap $1mm$, $h = 3mm$. Blue: $r_1 = 25mm, r_2 = 28mm, r_3 = 21mm, r_4 = 24mm$ Radial thickness $r_2 - r_1 = r_4 - r_3 = 3mm$, Green: Radial thickness $4mm$ , Red: Radial thickness $5mm$.

Moreover, the blue line on Fig.11 shows that the maximum force varies inversely to the square of the air gap radial dimension. Thus, the maximum axial force is very sensitive to the air gap radial dimension, which should be as small as possible to have large forces but which is generally set by the mechanical constraints of the device. As a remark, for ring magnets of $3 \times 3mm^2$ cross section, if the radial mechanical air gap has to be $2mm$, the axial force exerted is rather negligible!

## 4.2 Multiple ring structures: stacked structures

A remark of the previous section will be exploited now. Indeed, the study of the ring height shew that diminishing the magnet height, and thus its volume, could be done without a dramatical decrease of the force. Hence the idea of using rather short rings but of stacking them with alternate polarization directions to achieve larger forces.

For example, let's consider a stack of elementary devices of same dimensions as the previously considered devices: $r_1 = 25mm$, $r_2 = 28mm$, $r_3 = 21mm$, $r_4 = 24mm$, $h = 3mm$, cross section $3 \times 3mm^2$. The bottom of the first device is located at $z = 0$, the bottom of the second one at $z = 3$ and so on (Fig. 12).

Fig.13 shows the axial stiffness for the elementary device (blue), for a stack of two elementary devices (green) and for a stack of three elementary devices (red). The consequence of stacking is that the different axial stiffnesses are additive, as they all act in the same way. So, the total axial stiffness of the device increases more rapidly than the number of stacked devices (Yonnet et al., 1991). Indeed, the maximal stiffness for one ring pair with a square section of $3 \times 3mm^2$ is 30.8 N/mm, for two pairs 87.9 N/mm and for three pairs 140 N/mm. If $n$ is the number of pairs, the stiffness of a stack is approximately $2n - 1$ times greater than the stiffness of a pair.
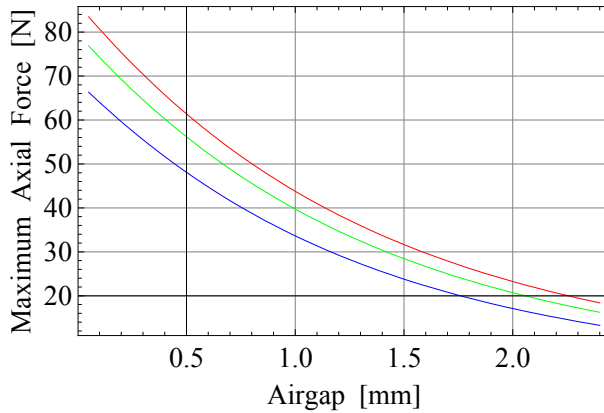
Fig. 11. Maximum axial force versus the air gap radial dimension for several ring radial thicknesses. $h = 3mm$. Blue: $r_1 = 25mm, r_2 = 28mm, r_3 = 21mm, r_4 = 24mm$ Radial thickness $r_2 - r_1 = r_4 - r_3 = 3mm$, Green: Radial thickness $4mm$ , Red: Radial thickness $5mm$.
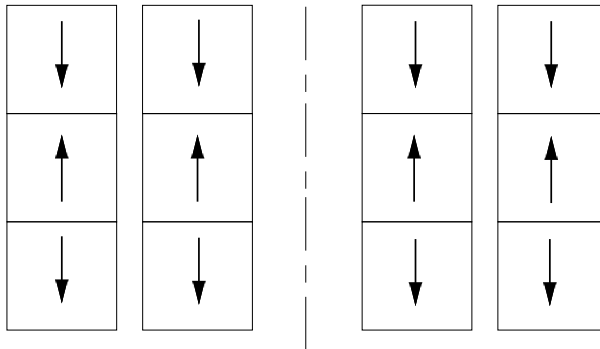


Fig. 12. Cross-section of a stack of three elementary devices with alternate axial polarizations.

Besides, the stiffness obtained for a ring pair of same total dimensions as the stack of three pairs is 34.7 N/mm. This example emphazises the advantage, for a given volume and a sufficient axial height, of splitting the ring into several rings of smaller heights and opposite polarizations: making three pairs increases the stiffness fourfold. The splitting is interesting as long as the height of each ring magnet is large enough (see section 4.1.3).

## 5. Study and characteristics of axial bearings with axially polarized ring magnets and a plane air gap.

This section considers devices with two axially polarized ring magnets of exactly the same dimensions. They are positioned so as to have the same rotation axis and thus are separated by a plane air gap. In this configuration, if the rings have the same polarization direction, the device works as a radial bearing, if the polarizations are opposite, it works as an axial bearing. It is noticeable that for axial polarizations, parallel polarizations yield
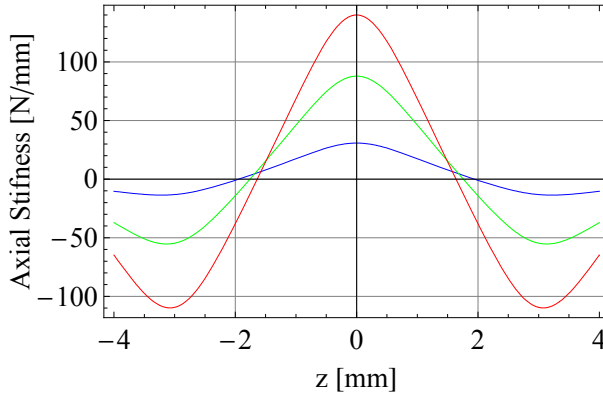
Fig. 13. Axial stiffness for one elementary device (blue), for a stack of two elementary devices (green) and three elementary devices (red).

radial bearings whereas antiparallel polarizations yield axial ones, whatever the air gap shape.

For these structures, the axial displacement of one ring corresponds to an air gap variation. Of course, the maximal axial force between the rings occurs when they are axially in contact with each other. When the air gap, $z$, increases, the axial force decreases, as show on Fig.15. As the variation is monotonous, the axial stiffness has always the same sign (Fig. 16) and the force the same nature (restoring, here).
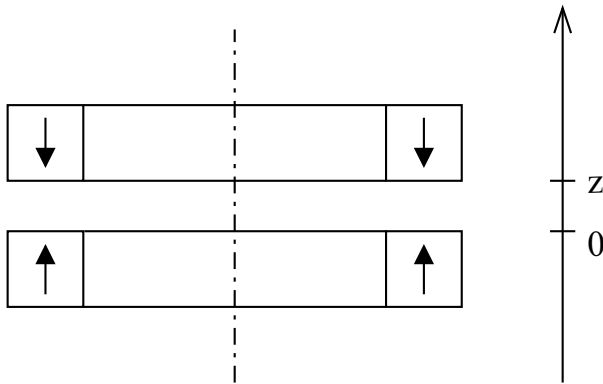


Fig. 14. Cross-section of a bearing with a plane air gap

Moreover, the axial force depends on the size of surfaces which are facing each other. Therefore, it is obvious that when the ring radial thickness increases, the force increases in the same way. The only other interesting parameter is the ring axial height. Figure 17 and 18 show how the axial force and stiffness vary when the air gap changes for different ring axial height. The force doesn't seem to vary greatly when the magnet height changes, and the stiffness even less. But the attention should be drawn to the scale of the force amplitude. Indeed, Fig.19 and 20 show the force and the stiffness for a fixed air gap when the magnet height varies.
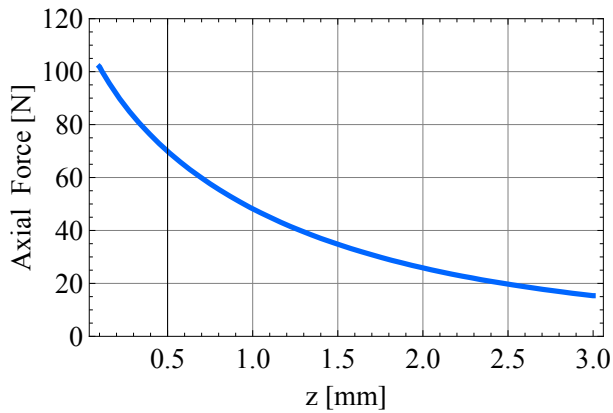
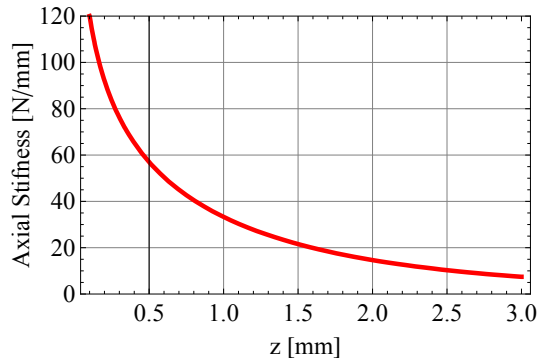Fig. 15. Axial force when the plane air gap length, $z$, varies. $r_1 = r_3 = 25mm, r_2 = r_4 = 28mm, h = 3mm$.



Fig. 16. Axial stiffness when the plane air gap length, $z$, varies. $r_1 = r_3 = 25mm, r_2 = r_4 = 28mm, h = 3mm$.

They emphazise the fact that increasing the magnet height is interesting for small heights, but becomes rapidly inefficient, especially with regard to the stiffness.

## 6. Determination of the force transmitted between two radially polarized ring permanent magnets.

The structure considered now is shown in Fig 21. The device is constituted by two concentric ring magnets which are separated by a cylindrical air gap and are radially polarized, their polarizations being in the same direction.

### 6.1 Notations

The parameters which describe the geometry of Fig.21 and its properties are listed below:
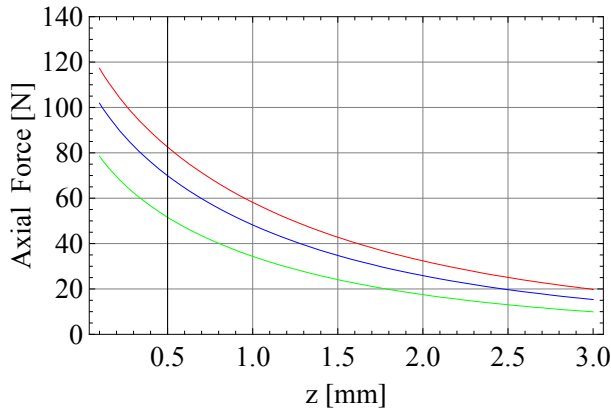$J_1$: outer ring polarization [T].
$J_2$: inner ring polarization [T].

Fig. 17. Axial force when the plane air gap length, $z$, varies. $r_1 = r_3 = 25mm$, $r_2 = r_4 = 28mm$. Blue: $h = 3mm$, Green: $h = 2mm$ , Red: $h = 4mm$.

$r_{in}$, $r_{out}$: radial coordinates of the outer ring [m].
$r_{in2}$, $r_{out2}$: radial coordinates of the inner ring [m].
$h$: outer ring height [m].
$z_b - z_a$: inner ring height [m].
The rings are radially centered and their polarizations are supposed to be uniformly radial.

## 6.2 Magnet modelling

For this kind of configuration, the coulombian model of magnets is the one that gives interesting analytical and semi analytical expressions. Consequently, each ring permanent magnet is represented by two curved planes which correspond to the inner and outer faces of the rings. These faces are charged with a surface magnetic pole density $\sigma^*$ and the charge balance is reached thanks to a magnetic pole volume density $\sigma_v^*$. For each ring, the inner face is charged with the surface magnetic pole density $+\sigma^*$ and the outer one is charged with the surface magnetic pole density $-\sigma^*$. Moreover, all the calculations are carried out with $\sigma^* = \vec{J}.\vec{n} = 1T$ where $\vec{J}$ is the magnetic polarization vector and $\vec{n}$ is the unit normal vector which is directed towards the rotation axis.

## 6.3 Expression of the force

The axial force exerted between the magnets results of the interaction of all the charge densities. The axial component of the magnetic field produced by the outer ring permanent magnet is $H_z$. Thus, the axial force $F_z$ can be written as follows:

$$F_z = \int \int_{(S_{in})} H_z \sigma_2^* d\tilde{S} - \int \int_{(S_{out})} H_z \sigma_2^* d\tilde{S} + \int \int \int_{(V)} H_z \frac{\sigma_2^*}{r_2} d\tilde{V} \qquad (17)$$

where $\sigma_2^*$ is the magnetic pole surface density of the inner ring magnet, $(S_{in})$ is the surface of the inner face of the inner ring permanent magnet, $(S_{out})$ is the surface of the outer face of the inner ring permanent magnet and $(V)$ is the volume of the inner ring permanent magnet. So,
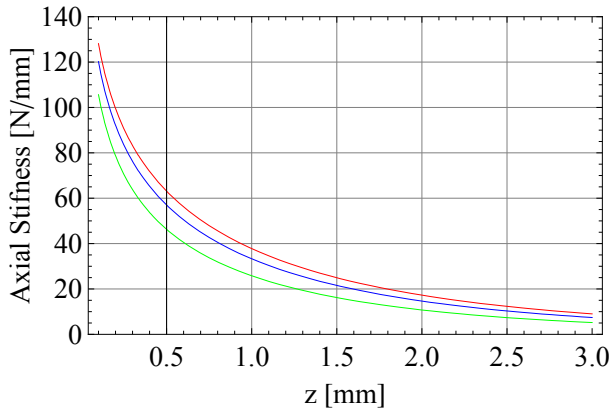
Fig. 18. Axial stiffness when the plane air gap length, $z$, varies. $r_1 = r_3 = 25mm$, $r_2 = r_4 = 28mm$. Blue: $h = 3mm$, Green: $h = 2mm$ , Red: $h = 4mm$.

the axial force $F_z$ can be expressed by:

$$
\begin{aligned}
F_z \ = \ & - \int_{\theta_1=0}^{2\pi} \int_{z_1=0}^{h} \int_{\theta_2=0}^{2\pi} \int_{z_2=z_a}^{z_b} a(r_{in}, r_{out2}) dz_1 d\theta_1 dz_2 d\theta_2 \\
& + \int_{\theta_1=0}^{2\pi} \int_{z_1=0}^{h} \int_{\theta_2=0}^{2\pi} \int_{z_2=z_a}^{z_b} a(r_{out}, r_{out2}) dz_1 d\theta_1 dz_2 d\theta_2 \\
& + \int_{\theta_1=0}^{2\pi} \int_{z_1=0}^{h} \int_{\theta_2=0}^{2\pi} \int_{z_2=z_a}^{z_b} a(r_{in}, r_{in2}) dz_1 d\theta_1 dz_2 d\theta_2 \\
& - \int_{\theta_1=0}^{2\pi} \int_{z_1=0}^{h} \int_{\theta_2=0}^{2\pi} \int_{z_2=z_a}^{z_b} a(r_{out}, r_{in2}) dz_1 d\theta_1 dz_2 d\theta_2 \\
& - \int_{r_1=r_{in}}^{r_{out}} \int_{\theta_1=0}^{2\pi} \int_{z_1=0}^{h} \int_{\theta_2=0}^{2\pi} \int_{z_2=z_a}^{z_b} b(r_{out2}, r_1) dr_1 dz_1 d\theta_1 dz_2 d\theta_2 \\
& + \int_{r_1=r_{in}}^{r_{out}} \int_{\theta_1=0}^{2\pi} \int_{z_1=0}^{h} \int_{\theta_2=0}^{2\pi} \int_{z_2=z_a}^{z_b} b(r_{in2}, r_1) dr_1 dz_1 d\theta_1 dz_2 d\theta_2 \\
& + \int_{r_2=r_{in2}}^{r_{out2}} \int_{\theta_1=0}^{2\pi} \int_{z_1=0}^{h} \int_{\theta_2=0}^{2\pi} \int_{z_2=z_a}^{z_b} b(r_{in}, r_2) dz_1 d\theta_1 dr_2 dz_2 d\theta_2 \\
& - \int_{r_2=r_{in2}}^{r_{out2}} \int_{\theta_1=0}^{2\pi} \int_{z_1=0}^{h} \int_{\theta_2=0}^{2\pi} \int_{z_2=z_a}^{z_b} b(r_{out}, r_2) dz_1 d\theta_1 dr_2 dz_2 d\theta_2 \\
& + \int_{r_1=r_{in}}^{r_{out}} \int_{r_2=r_{in2}}^{r_{out2}} \int_{\theta_1=0}^{2\pi} \int_{z_1=0}^{h} \int_{\theta_2=0}^{2\pi} \int_{z_2=z_a}^{z_b} c(r_1, r_2) dr_1 dz_1 d\theta_1 dr_2 dz_2 d\theta_2
\end{aligned}
\tag{18}
$$

with

$$
a(\alpha, \beta) = \frac{\sigma_1^* \sigma_2^*}{4\pi\mu_0} \frac{(z_2 - z_1)\alpha\beta}{(\alpha^2 + \beta^2 - 2\alpha\beta + (z_2 - z_1)^2)^{\frac{3}{2}}}
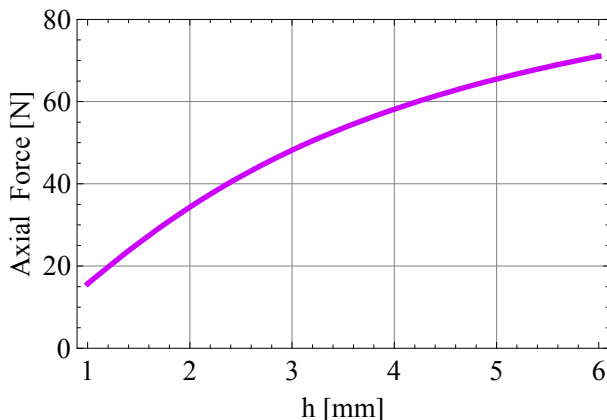\tag{19}
$$

Fig. 19. Axial force when the ring axial height, $h$, varies. Plane air gap $z = 1mm$, $r_1 = r_3 = 25mm$, $r_2 = r_4 = 28mm$.

where $\sigma_1^*$ is the magnetic pole surface density of the outer ring magnet. and

$$b(\alpha, \beta) = \frac{a(\alpha, \beta)}{\beta} \tag{20}$$

$$c(\alpha, \beta) = \frac{a(\alpha, \beta)}{\alpha \beta} \tag{21}$$

The next step is to evaluate Eq. (18). Therefore, the number of integrals is first reduced by integrating analytically $a(\alpha, \beta)$, $b(\alpha, \beta)$ and $c(\alpha, \beta)$ according to the integral variables. Unfortunately, a fully analytical expression of the force can't be found but the following semi-analytical expression is quite useful:

$$
\begin{aligned}
F_z &= \frac{\sigma_1^* \sigma_2^*}{2\mu_0} \int_{\theta_1=0}^{2\pi} S d\theta_1 \\
&+ \frac{\sigma_1^* \sigma_2^*}{2\mu_0} \int_{\theta_1=0}^{2\pi} M d\theta_1 \\
&+ \frac{\sigma_1^* \sigma_2^*}{2\mu_0} \int_{\theta_1=0}^{2\pi} \int_{r_2=r_{in2}}^{r_{out2}} V d\theta_1 dr_2
\end{aligned}
\tag{22}
$$

where $S$ represents the interaction between the magnetic pole surface densities of each ring magnet, $M$ corresponds to the magnetic interaction between the magnetic pole surface densities of one ring permanent magnet and the magnetic pole volume density of the other one, and $V$ denotes the interaction between the magnetic pole volume densities of each ring permanent magnet.

# Thank You for previewing this eBook

You can read the full version of this eBook in different formats:

- ➢ HTML (Free /Available to everyone)

- ➢ PDF / TXT (Available to V.I.P. members. Free Standard members can access up to 5 PDF/TXT eBooks per month each month)

- ➢ Epub & Mobipocket (Exclusive to V.I.P. members)

To download this full book, simply select the format you desire below